

Journal of Applied Remote Sensing

Remote sensing of fuel moisture content from canopy water indices and normalized dry matter index

E. Raymond Hunt, Jr.
Lingli Wang
John J. Qu
Xianjun Hao



Remote sensing of fuel moisture content from canopy water indices and normalized dry matter index

E. Raymond Hunt Jr.,^a Lingli Wang,^b John J. Qu,^b and Xianjun Hao^b

^aHydrology and Remote Sensing Laboratory, U.S. Department of Agriculture–Agricultural Research Service, 10300 Baltimore Avenue, Beltsville, Maryland 20705-2325

Raymond.Hunt@ars.usda.gov

^bGeorge Mason University, Department of Geography and Geoinformation Sciences, 4400 University Avenue, Fairfax, Virginia 22030-4444

Abstract. Fuel moisture content (FMC), an important variable for predicting the occurrence and spread of wildfire, is the ratio of foliar water content and foliar dry matter content. One approach for the remote sensing of FMC has been to estimate the change in canopy water content over time by using a liquid-water spectral index. Recently, the normalized dry matter index (NDMI) was developed for the remote sensing of dry matter content using high-spectral-resolution data. The ratio of a spectral water index and a dry matter index corresponds to the ratio of foliar water and dry matter contents; therefore, we hypothesized that FMC may be remotely sensed with a spectral water index divided by NDMI. For leaf-scale simulations using the PROSPECT (leaf optical properties spectra) model, all water index/NDMI ratios were significantly related to FMC with a second-order polynomial regression. For canopy-scale simulations using the SAIL (scattering by arbitrarily inclined leaves) model, two water index/NDMI ratios, with numerators of the normalized difference infrared index (NDII) and the normalized difference water index (NDWI), predicted FMC with R^2 values of 0.900 and 0.864, respectively. Leaves from three species were dried or stacked to vary FMC; measured NDII/NDMI was best related to FMC. Whereas the planned NASA mission Hyperspectral Infrared Imager (HypIRI) will have high spectral resolution and very high signal-to-noise properties, the planned 19-day repeat frequency will not be sufficient for monitoring FMC with NDII/NDMI. Because increased fire frequency is expected with climatic change, operational assessment of FMC at large scales may require polar-orbiting environmental sensors with narrow bands to calculate NDMI. © 2012 Society of Photo-Optical Instrumentation Engineers (SPIE). [DOI: [10.1117/1.JRS.6.061705](https://doi.org/10.1117/1.JRS.6.061705)]

Keywords: normalized dry matter content; normalized dry matter index; PROSPECT; SAIL; normalized difference infrared index; normalized difference water index.

Paper 12310SSP received Sep. 17, 2012; revised manuscript received Nov. 5, 2012; accepted for publication Nov. 12, 2012; published online Dec. 3, 2012.

1 Introduction

In the mid-1980s, there was a large increase in the frequency and duration of large wildfires in the western United States associated with springtime and summertime air temperature.¹ Future changes in climate are expected to dramatically increase wildfires,^{2,3} and increases in wildfires will have a positive feedback on climatic change by increasing various radiative forcings compared to preindustrial times.⁴ Adaption and mitigation strategies at regional scales may depend on predicting fire behavior with simulation models. Fuel moisture content (FMC) is one of the main parameters for predicting the occurrence and spread of wildfire.^{5,6}

FMC, the mass of water per unit mass of dry matter in vegetation, is determined simply from fresh and oven-dry weights. However, large numbers of samples are required for estimating FMC over large areas, so many studies have examined different methods for the remote sensing of FMC.^{7–15} Remotely sensed indices that estimate foliar liquid-water content are generally correlated with FMC,^{9,11,12,14} the major problem is determination of the dry matter content in fresh leaves. Currently, a promising biophysical approach is the retrieval of both water and dry matter

contents by inverting leaf and canopy radiative-transfer models.^{13–15} However, model inversions are “ill-posed problems” because different combinations of parameters may produce similar reflectance spectra.¹⁵ An alternative is to use spectral indices for liquid water content and a spectral index for dry matter content.^{16–18}

The normalized dry matter index (NDMI) was developed by examining spectral reflectances of fresh leaves across a wide range of species:^{16,17}

$$\text{NDMI} = (\rho_{1649} - \rho_{1722}) / (\rho_{1649} + \rho_{1722}), \quad (1)$$

where ρ_{1649} and ρ_{1722} are the spectral reflectances at 1649- and 1722-nm wavelength, respectively. NDMI is based on absorption by the C—H bond stretch overtone at 1722 nm;¹⁹ C—H bonds are found in all leaf biochemical constituents: lipids, proteins, nucleic acids, lignin, cellulose, and other carbohydrates. Because foliar FMC is the ratio of leaf water content and dry matter content, we hypothesized that the ratio of a liquid-water spectral index with NDMI would estimate FMC.

With a ratio of two indices, many of the factors that affect vegetation indices in general, such as leaf area index (LAI) and leaf angle distribution (LAD), may be hypothesized to cancel out, resulting in a consistent estimate of FMC. There have been a large number of spectral indices for liquid water content presented in the literature, a few of which are presented in Table 1. To avoid spurious correlations, an ideal index for water should not be correlated to NDMI; because both dry matter and water absorb radiation between 1600 and 1800 nm [Fig. 1(a)], changes in one biophysical parameter could be attributed mistakenly to the other parameter. To reduce the

Table 1 Remotely sensed indices related to leaf and canopy water content.

Index	Abbreviation	Formula	Reference
Normalized difference infrared index	NDII	$(\rho_{860} - \rho_{1650}) / (\rho_{860} + \rho_{1650})$	20
Reciprocal of moisture stress index	RMSI	ρ_{860} / ρ_{1650}	21
Normalized difference water index	NDWI	$(\rho_{860} - \rho_{1240}) / (\rho_{860} + \rho_{1240})$	22
Simple ratio water index	SRWI	ρ_{860} / ρ_{1240}	23

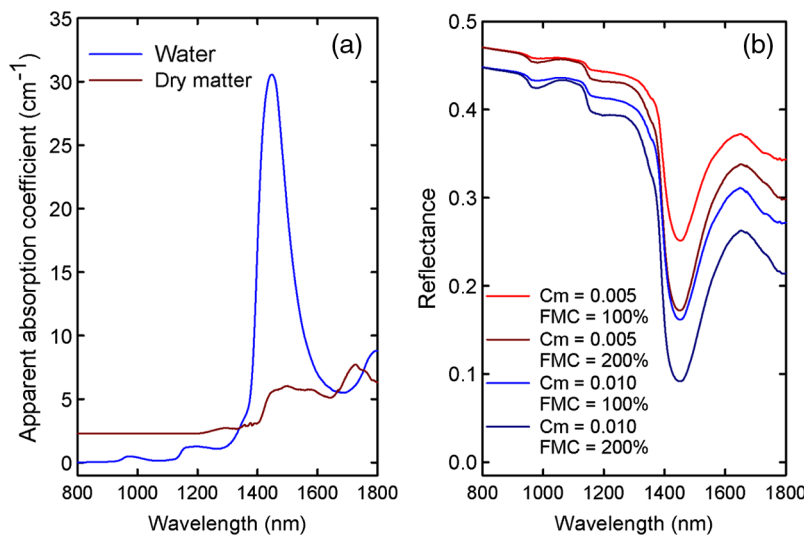


Fig. 1 (a) Spectral absorption coefficients for water and dry matter used in the PROSPECT leaf model. (b) Four model simulations with FMC = 1.0 and 2.0, and $C_m = 0.005$ and 0.010 g cm^{-2} . The leaf structure parameter N was 1.5 for all simulations. From the top to bottom spectra, the differences in reflectance between 1649 to 1722 nm wavelength are 0.019, 0.021, 0.028, and 0.030, respectively.

occurrence of spurious correlations, we compared FMC to ratios of spectral water indices with NDMI using both radiative-transfer model simulations and laboratory spectral reflectance measurements.

2 Methods

2.1 Calculation of FMC and Remote Sensing Indices

FMC (dimensionless) was calculated from leaf water content C_w (g cm^{-2}) and leaf dry matter content C_m (g cm^{-2}):

$$C_w = (W_f - W_d)/A, \quad (2)$$

$$C_m = W_d/A, \quad (3)$$

and

$$\text{FMC} = (W_f - W_d)/W_d = C_w/C_m, \quad (4)$$

where W_f is leaf fresh weight (g), W_d the leaf dry weight (g), and A the leaf area (cm^2). Canopy water content and canopy dry matter content were the leaf C_w and C_m multiplied LAI, respectively. However, the ratio $C_w:C_m$ was used for both leaves and canopies because leaf area canceled out.

Four vegetation water indices were selected for analysis based on two different water absorption bands (1240 and 1650 nm) and two different methods for index calculation (normalized difference and ratio) (Table 1). The indices were the normalized difference infrared index (NDII),²⁰ the reciprocal of moisture stress index (RMSI),²¹ the normalized difference water index (NDWI),²² and the simple ratio water index (SRWI).²³ RMSI was used instead of the moisture stress index (Table 1) because RMSI increases with increasing FMC, allowing for better comparisons among the combined index ratios.

2.2 PROSPECT and SAIL Model Simulations

The leaf radiative-transfer model, PROSPECT (leaf optical properties spectra) version 4,^{24,25} was used to simulate leaf reflectance and transmittance [Fig. 1(b)]. For a total of 250 simulations, all input parameters except chlorophyll content were randomly generated using a uniform distribution within given range of each variable (Table 2). Total chlorophyll a and b content (C_{ab}) was held constant at $40 \mu\text{g cm}^{-2}$, because there was no effect of C_{ab} on shortwave-infrared reflectances. The range of each input parameter (Table 2) was reasonable.²⁶ However, C_w and C_m are somewhat correlated: leaves with high C_w usually have high C_m . Random combinations of C_w and C_m created a larger range of FMC than would naturally occur.

The scattering by arbitrarily inclined leaves (SAIL) model²⁷ was used to simulate canopy spectral reflectance as a function of leaf reflectance and transmittance, soil background reflectance, LAI, and LAD (Table 2). Leaf spectral reflectances and transmittances from the PROSPECT simulations were used as inputs to the SAIL model. The spectral reflectance of a dry Othello silt loam (fine silty, mixed, active, mesic Typic Endoaquult) from Salisbury, Maryland, was used for the background. A total of 4500 simulations were made ($3 \text{ LAD} \times \text{LAI} \times 250 \text{ PROSPECT simulations}$).

2.3 Spectral Reflectance Measurements

Leaves of *Quercus alba* (white oak), *Acer rubrum* (red maple), and *Zea mays* (maize) were collected at the U.S. Department of Agriculture–Agricultural Research Service, Beltsville Agricultural Research Center, Beltsville, Maryland. The leaves were placed into plastic bags and then into an insulated chest, to minimize water loss during transport to the laboratory. Leaf spectral reflectances of the adaxial surface were measured with an Analytical Spectral Devices FieldSpec

Table 2 Input parameters for PROSPECT leaf model and SAIL canopy model simulations.

Model	Model and parameters	Values
PROSPECT ($n = 250$)	Leaf structure parameter (N)	1 to 3
	Chlorophyll content (C_{ab} , $\mu\text{g cm}^{-2}$)	40
	Water content (C_w , g cm^{-2})	0.004 to 0.034
	Dry matter content (C_m , g cm^{-2})	0.002 to 0.018
SAIL ($n = 4500$)	Leaf area index (LAI)	1.0, 1.5, 2.0, 3.0, 5.0, 6.0
	Leaf angle distribution (LAD)	Erectophile, planophile, and spherical
	Fraction of direct solar irradiance	0.8
	Background reflectance	Othello silt-loam
	Solar declination	0 deg
	Latitude	36 deg
	View zenith angle	Nadir
	Time of day	10:00 a.m.

Pro FR Spectroradiometer (Analytical Spectral Devices, Boulder, Colorado) and an LI-1800-12 Integrating Sphere (LiCor, Lincoln, Nebraska). Leaf fresh and dry weights were measured using an analytical balance (accurate to 0.1 mg), and leaf area was measured with a LiCor LI-3100c Area Meter.

Measurements of fresh weight, area, and spectral reflectances were made on single leaves of *Q. alba*, *A. rubrum*, and *Z. mays* immediately upon return to the laboratory. Stacks of two and three leaves of white oak and red maple were measured to simulate a planophile canopy. Then, the leaves were placed on a laboratory bench to lose water. At frequent intervals (about 30 to 45 min), fresh weight and spectral reflectances were measured at the same spot on the leaves. Finally, the leaves were placed in an oven at 50°C for 24 h; leaf dry weight was measured to calculate C_w , C_m , and FMC [Eqs. (2)–(4)].

2.4 Statistical Approaches

Polynomial regressions were used to quantify the relationship between FMC and spectral water indices divided by NDMI:

$$\text{FMC} = b_2(\text{index}/\text{NDMI})^2 + b_1(\text{index}/\text{NDMI}) + b_0, \quad (5)$$

where b_2 , b_1 , and b_0 were the regression coefficients, and *index* was either NDII, NDWI, RMSI, or SRWI (Table 1). The performance of each water index was evaluated by the coefficient of determination (R^2) and the root mean square error (RMSE).

Two components of RMSE, systematic and unsystematic (RMSE_s and RMSE_u , respectively), were calculated to evaluate model performance from the PROSPECT simulations when applied to leaf reflectance data.²⁸

3 Results

3.1 SAIL and PROSPECT Model Simulations

The effect of dry matter content on leaf spectral reflectance using the PROSPECT model was small [Fig. 1(b)]; the slopes from about 1700 to 1800 nm were more negative with $C_m = 0.010 \text{ g cm}^{-2}$ compared to the slopes where $C_m = 0.005 \text{ g cm}^{-2}$. There was also an effect

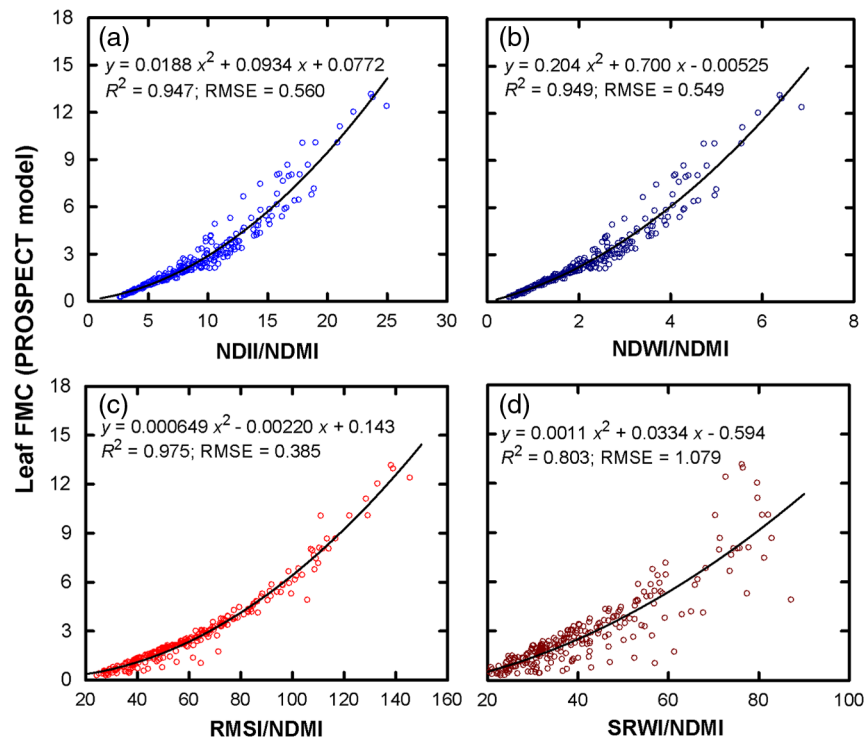


Fig. 2 Simulated leaf fuel moisture content (FMC) versus the ratio of four different water indices with the normalized dry matter index (NDMI) from PROSPECT model simulations ($n = 250$). The black lines are the polynomial regressions shown in each panel.

of dry matter on the near-infrared reflectances from about 800 to 1200 nm wavelength [Fig. 1(b)], because the absorption coefficients for dry matter were larger than those of water [Fig. 1(a)]. However, the most sensitive parameter in PROSPECT is the leaf structure parameter N , which was held constant at 1.5 in Fig. 1(b). Variations in N would cause much larger changes in near-infrared reflectance, so the effect of dry matter would not be apparent in the near infrared. Absolute changes in reflectance caused by differences in leaf water content were largest at about 1450 nm, but at this wavelength, little solar radiation (if any) reaches Earth's surface because of atmospheric water vapor.²⁹

From the PROSPECT model simulations, ratios of the four spectral water indices with NDMI worked well for predicting FMC (Fig. 2). Second-order polynomial regressions fitted the data better than linear regressions. The R^2 values were >0.9 , except for SRWI/NDMI, which had an R^2 of 0.803 [Fig. 2(d)]. RMSI/NDMI had the highest R^2 and lowest RMSE predicting FMC over the range of inputs [Fig. 2(c)]. However, FMC between 0.5 and 1.0 is the important range for monitoring FMC,¹¹ and RMSI/NDMI had more variation in this smaller range of FMC [Fig. 2(c)].

At the canopy scale with SAIL-simulated canopy reflectances, the relationships among FMC with the *index*/NDMI ratios showed much more scatter (Fig. 3) compared to the leaf-level simulations. Second-order polynomial regressions also provided the best fit for each vegetation water index (Fig. 3, black lines). NDII/NDMI and NDWI/NDMI had higher R^2 and had positive coefficients for the second-order term, similar to the PROSPECT simulations [Fig. 3(a) and 3(b)]. Both ratio-based spectral water indices divided by NDMI, i.e., RMSI/NDMI and SRWI/NDMI, had negative coefficients for the squared term [Fig. 3(c) and 3(d)].

Because leaf area was assumed to cancel out of the calculation for canopy FMC, we tested the hypothesis that the regression models from the PROSPECT simulations (Fig. 3, green lines) would fit the results from the SAIL model simulations. Regression equations between FMC and NDII/NDMI and NDWI/NDMI from the SAIL model predicted higher FMC compared to the leaf-level simulations [Fig. 3(a) and 3(b)]. On the other hand, the regression equations from the PROSPECT simulations fit the results from the SAIL model simulations for RMSI/NDMI and SRWI/NDMI almost as well as the polynomial regressions [Fig. 3(c) and 3(d)], because of

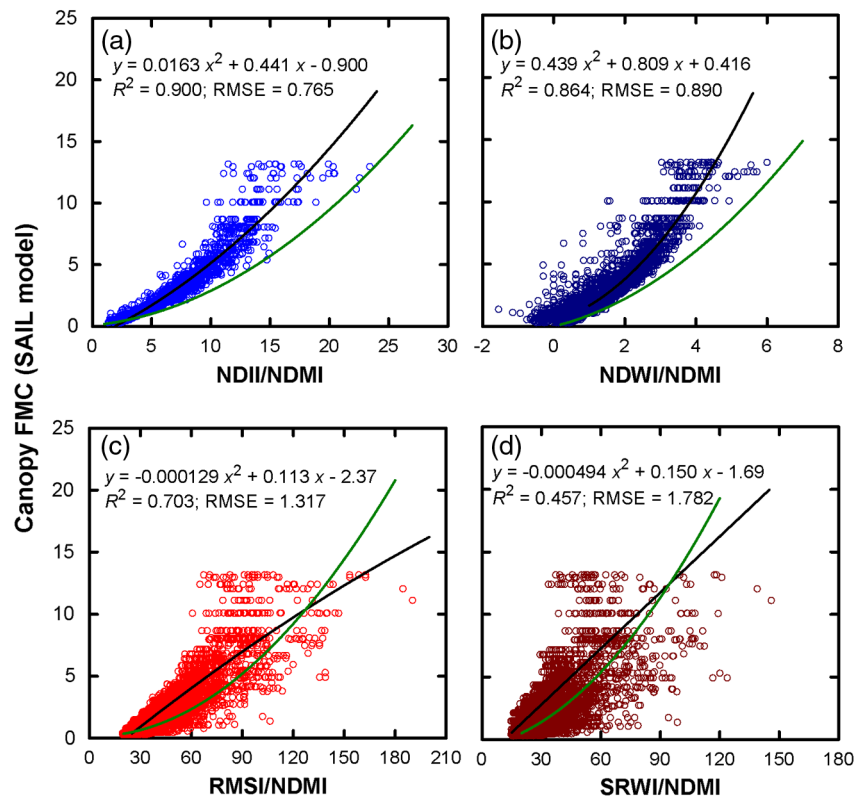


Fig. 3 Simulated canopy FMC versus the ratio of four water indices with NDMI using the SAIL model ($n = 4500$). The black lines are the polynomial regression equations shown in each panel and the green lines are the polynomial regression equations from the PROSPECT model simulations (Fig. 2).

the large amounts of scatter. Therefore, leaf-level simulations with the PROSPECT model could not be used to predict FMC at the canopy scale.

3.2 Measurements on Drying Leaves and Leaf Stacks

Using the pooled leaf and leaf-stack data, there was a strong positive correlation between NDMI and C_m and a significant negative correlation between NDMI and C_w (Table 3). In contrast, the spectral water indices were correlated to C_w and were not correlated to C_m . Furthermore, the spectral water indices had higher correlations with C_w compared to FMC (Table 3), so spectral

Table 3 Correlations of individual water and dry matter spectral indices from reflectances of drying leaves of *Quercus alba*, *Acer rubrum*, and *Zea mays*, and from leaf stacks of *Q. alba* and *A. rubrum* ($n = 242$).

Index or index ratio	Dry matter content (C_m)	Water content (C_w)	Fuel moisture content (FMC)
NDMI	0.726	-0.262	-0.562
NDII	-0.0429	0.599	0.299
RMSI	-0.038	0.426	0.251
NDWI	-0.00133	0.419	0.263
SWRI	-0.040	0.398	0.243

Note: Stacks of 2 or 3 leaves have the same FMC but higher C_w and C_m compared to single leaves. Critical values of r are 0.123 for $P = 0.95$ and 0.165 for $P = 0.99$.

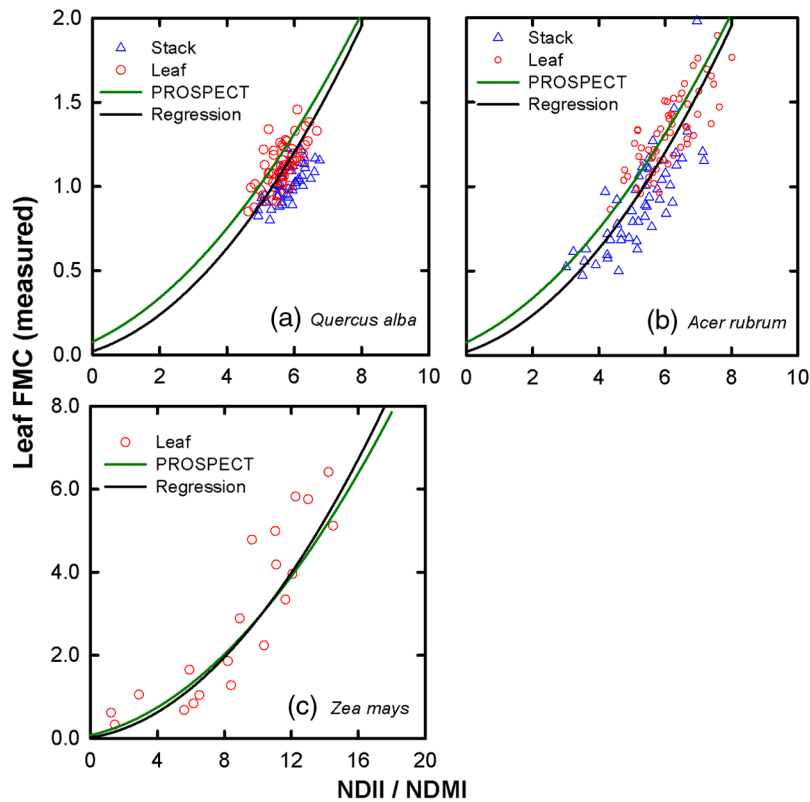


Fig. 4 Measured FMC versus NDII/NDMI calculated from spectral reflectance measurements for individual leaves of *Q. alba* (a), *A. rubrum* (b), and *Z. mays* (c) and for leaf stacks of *Q. alba* (a) and *A. rubrum* (b). The black lines show the pooled polynomial regression combining the five datasets (Table 3) and the green lines show the regression equation from the PROSPECT simulations [Fig. 2(a)].

water indices alone were not good predictors of FMC. Correlations between FMC and ratios of two spectral indices, one for leaf liquid water and NDMI for leaf dry matter, were not spurious because the experimental design reduced potential autocorrelation. Normally, C_w and C_m would be highly correlated because both C_w and C_m depend on leaf thickness.

Leaves of *Z. mays* had a much larger range in FMC (from 0.03 to 6.4) compared to leaves of *Q. alba* and *A. rubrum* (Fig. 4), because the leaves of *Z. mays* had much less dry weight per leaf area and, presumably, less structural tissue. With single-leaf and stacked-leaf datasets combined, FMC was best predicted with a second-order polynomial regression (Table 4). NDII/NDMI had the highest R^2 and the lowest RMSE, whereas SRWI/NDMI had the lowest R^2 and highest RMSE (Table 4).

Table 4 Polynomial regression coefficients and statistics for pooled leaf and leaf-stack data for all species.

Index	b_2	b_1	b_0	R^2	RMSE
NDII/NDMI	0.0221	0.0644	0.0210	0.853	0.306
NDWI/NDMI	0.596	-0.701	1.03	0.769	0.383
RMSI/NDMI	0.000410	-0.0143	0.860	0.659	0.466
SRWI/NDMI	0.000404	-0.000594	0.628	0.485	0.572

Note: Leaves and leaf stacks were slowly dried to create differences in FMC. The polynomial equation is $FMC = b_2(\text{index}/NDMI)^2 + b_1(\text{index}/NDMI) + b_0$ ($n = 242$).

Table 5 Comparison of RMSE and component terms (systematic RMSE_s and unbiased RMSE_u) of leaf and stacked-leaf datasets using predicted FMC from the pooled polynomial regression using measured NDII/NDMI (Table 3) and the polynomial regression from the PROSPECT model simulations [Fig. 1(a)], respectively.

Dataset	Pooled data regression			PROSPECT regression		
	RMSE	RMSE _s	RMSE _u	RMSE	RMSE _s	RMSE _u
<i>Q. alba</i> leaves	0.116	0.027	0.118	0.137	0.133	0.116
<i>Q. alba</i> leaf stack	0.162	0.038	0.137	0.256	0.160	0.129
<i>A. rubrum</i> leaves	0.178	0.034	0.176	0.165	0.097	0.168
<i>A. rubrum</i> leaf stack	0.195	0.065	0.175	0.259	0.200	0.171
<i>Z. mays</i> leaves	0.910	0.381	0.839	0.919	0.652	0.639

The pooled regression equation from the combined single-leaf and stacked-leaf datasets for NDII/NDMI (Table 4) predicted FMC accurately for each dataset (Fig. 3) with relatively low RMSE (Table 5). The unsystematic RMSE was greater than systematic RMSE for each data regression. The polynomial regressions from the PROSPECT simulations also predicted FMC with relatively low RMSE; systematic and unsystematic RMSE were about equal (Table 5). Leaves of *Z. mays* had the highest RMSE_s for predicted FMC from the pooled-data regression and the PROSPECT regression.

4 Discussion

In general, vegetation indices are sensitive to several different attributes of plant canopies. Ratios of two indices, one more strongly related to leaf chlorophyll content and one more strongly related to LAI, were originally tested for estimating crop nitrogen status in fields with variable LAI.^{30–33} As hypothesized, ratios of spectral water indices and NDMI were better correlated to FMC than were the individual indices.

Overall, the normalized difference water indices predicted FMC better than the ratio-based water indices for the same wavelength: NDII versus RMSI and NDWI versus SRWI. There is a nonlinear relationship between normalized difference and ratio-based indices:

$$\left[\frac{(x-y)}{(x+y)} \right] = \left[\frac{(x-y)/x}{(x+y)/x} \right] = \left[\frac{(1-y/x)}{(1+y/x)} \right], \quad (6)$$

where x and y are variables. So normalized difference indices for leaf water content are statistically more linear with respect to water content compared to ratio-based indices for water content. Whereas indices based on 1650-nm wavelength (e.g., NDII) performed similarly to indices based on 1240-nm wavelength (e.g., NDWI) in the PROSPECT model simulations [Fig. 2(a) and 2(b)], NDII performed better using the SAIL model simulations [Fig. 3(a) and 3(b)] and the experimental datasets (comparison not shown). NDII and related indices have been used to estimate the canopy water content for different land cover types,^{34–38} so it is reasonably well tested. However, NDII is also an important index for the remote sensing of snow cover and flooded areas;^{39,40} thus, using NDII to monitor FMC requires masking of nonvegetated land-cover types.

The signal for dry matter content was weaker than that of water content over much of the shortwave infrared, in part because the amount of dry matter in most fresh leaves is less than the amount of water²⁶ and in part because the absorption coefficient for dry matter is less than that of water.^{24,25} However, at about 1722 nm wavelength, the absorption coefficient of dry matter in the PROSPECT model is slightly greater than that of water, which was why this wavelength was selected for NDMI.^{16,17} The biggest problem in determining NDMI with remotely sensed data is the requirement for a narrow-band sensor with a very high signal-to-noise ratio in the shortwave infrared.

NASA is planning the Hyperspectral Infrared Imager (HyspIRI) mission with a launch after 2020; the hyperspectral sensor on-board HyspIRI is expected to have 60-m pixels and a 19-day repeat cycle. The spectral and radiometric qualities of HyspIRI are excellent for determining FMC, with either radiative model inversion or ratios of two indices, but the temporal repeat frequency is too low for monitoring changes in FMC for wildfire prediction. Except for a few species with large temporal variation of C_m , most of the variation in FMC would be caused by either changes in LAI or changes in C_w . The Moderate Resolution Imaging Spectroradiometer (MODIS) and the Visible Infrared Imaging Radiometer Suite (VIIRS) sensors do not have a narrow band at about 1722-nm wavelength for detecting canopy dry matter content, but MODIS and VIIRS have several bands with which spectral water indices could be calculated. With both seasonal HyspIRI data and frequent VIIRS data, canopy FMC could potentially be monitored at high temporal resolution for assimilation into wildfire models. However, based on current research, sensor-data fusion requires the sensors to have bands at similar wavelengths;⁴¹ fusion of two independently derived biophysical data products is more difficult because of the nonlinear responses between reflectances and biophysical variables.

In conclusion, a ratio of a spectral water index and a spectral dry matter index was strongly related to FMC at both leaf and canopy scales, so our primary hypothesis was supported. However, the polynomial equations of simulated NDII/NDMI and FMC were different at the leaf and canopy scales, even though the leaf spectral reflectances and transmittances from the PROSPECT leaf simulations were used in the SAIL canopy simulations. Therefore, the hypothesis that canopy variables, such as LAI and LAD, would cancel out was not supported. For monitoring FMC, there is no requirement for an imaging spectrometer *per se*; the requirement is for a narrow band at 1722 nm. Thus, operational monitoring for FMC may require a new sensor for optimum sensitivity to FMC.

Acknowledgments

The U.S. Department of Agriculture (USDA) prohibits discrimination in all its programs and activities on the basis of race, color, national origin, age, disability, and, where applicable, sex, marital status, familial status, parental status, religion, sexual orientation, genetic information, political beliefs, reprisal, or because all or part of an individual's income is derived from any public assistance program. (Not all prohibited bases apply to all programs.) Persons with disabilities who require alternative means for communication of program information (Braille, large print, audiotape, etc.) should contact USDA's TARGET Center at (202) 720-2600 (voice and TDD). To file a complaint of discrimination, write to USDA, Director, Office of Civil Rights, 1400 Independence Avenue, S.W., Washington, D.C. 20250-9410, or call (800) 795-3272 (voice) or (202) 720-6382 (TDD). USDA is an equal opportunity provider and employer.

References

1. A. L. Westerling et al., "Warming and earlier spring increase Western U.S. Forest Wildfire Activity," *Science* **313**(5789), 940–943 (2006), <http://dx.doi.org/10.1126/science.1128834>.
2. M. D. Flannigan et al., "Implications of changing climate for global wildland fire," *Int. J. Wildland Fire* **18**(5), 483–507 (2009), <http://dx.doi.org/10.1071/WF08187>.
3. O. Pechony and D. T. Schindell, "Driving forces of global wildfires over the past millennium and the forthcoming century," *Proc. Nat. Acad. Sci. U. S. A.* **107**(45), 19167–19170 (2010), <http://dx.doi.org/10.1073/pnas.1003669107>.
4. D. M. J. S. Bowman et al., "Fire in the earth system," *Science* **324**(5926), 481–484 (2009), <http://dx.doi.org/10.1126/science.1163886>.
5. M. G. Rollins, R. E. Keane, and R. A. Parsons, "Mapping fuels and fire regimes using remote sensing, ecosystem simulation, and gradient modeling," *Ecol. Appl.* **14**(1), 75–95 (2004), <http://dx.doi.org/10.1890/02-5145>.
6. R. E. Keane et al., "A method for mapping fire hazard and risk across multiple scales and its application in fire management," *Ecol. Model.* **221**(1), 2–18 (2010), <http://dx.doi.org/10.1016/j.ecolmodel.2008.10.022>.

7. R. E. Burgan, R. A. Hartford, and J. C. Eidenshink, "Using NDVI to assess departure from average greenness and its relation to fire business," Intermountain Research Station General Technical Report INT-GTR-333, USDA Forest Service, Washington, DC (1996).
8. C. C. Hardy and R. E. Burgan, "Evaluation of NDVI for monitoring live moisture in three vegetation types of the Western U.S.," *Photogramm. Eng. Remote Sens.* **65**(5), 603–610 (1999).
9. E. Chuvieco et al., "Estimation of fuel moisture content from multitemporal analysis of Landsat Thematic Mapper reflectance data: applications in fire danger assessment," *Int. J. Remote Sens.* **23**(11), 2145–2162 (2002), <http://dx.doi.org/10.1080/01431160110069818>.
10. E. Chuvieco et al., "Design of an empirical index to estimate fuel moisture content from NOAA-AVHRR images in forest fire danger studies," *Int. J. Remote Sens.* **24**(8), 1621–1637 (2003).
11. P. E. Dennison et al., "Use of normalized difference water index for monitoring live fuel moisture," *Int. J. Remote Sens.* **26**(5), 1035–1042 (2005), <http://dx.doi.org/10.1080/0143116042000273998>.
12. D. A. Roberts et al., "Evaluation of Airborne Visible/Infrared Imaging Spectrometer (AVIRIS) and Moderate Resolution Imaging Spectrometer (MODIS) measures of live fuel moisture and fuel condition in a shrubland ecosystem in Southern California," *J. Geophys. Res.* **111**, G04S02 (2006), <http://dx.doi.org/10.1029/2005JG000113>.
13. D. Riaño et al., "Estimation of fuel moisture content by inversion of radiative transfer models to simulate equivalent water thickness and dry matter content: analysis at leaf and canopy level," *IEEE Trans. Geosci. Remote Sens.* **43**(4), 819–826 (2005), <http://dx.doi.org/10.1109/TGRS.2005.843316>.
14. M. Yebra, E. Chuvieco, and D. Riaño, "Estimation of live fuel moisture content from MODIS images for fire risk assessment," *Agric. For. Meteorol.* **148**(4), 523–536 (2008), <http://dx.doi.org/10.1016/j.agrformet.2007.12.005>.
15. M. Yebra and E. Chuvieco, "Linking ecological information and radiative transfer models to estimate fuel moisture content in the Mediterranean region of Spain: solving the ill-posed inverse problem," *Remote Sens. Environ.* **113**(11), 2403–2411 (2009), <http://dx.doi.org/10.1016/j.rse.2009.07.001>.
16. L. Wang et al., "Towards estimation of canopy foliar biomass with spectral reflectance measurements," *Remote Sens. Environ.* **115**(3), 836–840 (2011), <http://dx.doi.org/10.1016/j.rse.2010.11.011>.
17. L. Wang et al., "Estimating dry matter content from spectral reflectance for green leaves of different species," *Int. J. Remote Sens.* **32**(22), 7097–7109 (2011), <http://dx.doi.org/10.1080/01431161.2010.494641>.
18. A. Romero, I. Aguado, and M. Yebra, "Estimation of dry matter content in leaves using normalized indexes and PROSPECT model inversion," *Int. J. Remote Sens.* **33**(2), 396–414 (2012), <http://dx.doi.org/10.1080/01431161.2010.532819>.
19. D. L. Peterson and G. S. Hubbard, "Scientific issues and potential remote-sensing requirements for plant biochemical content," *J. Imag. Sci. Tech.* **36**(5), 446–456 (1992).
20. M. A. Hardisky, V. Klemas, and R. M. Smart, "The influences of soil salinity, growth form, and leaf moisture on the spectral reflectance of *Spartina alterniflora* canopies," *Photogramm. Eng. Remote Sens.* **49**(1), 77–83 (1983).
21. E. R. Hunt, Jr. and B. N. Rock, "Detection of changes in leaf water content using near- and middle-infrared reflectance," *Remote Sens. Environ.* **30**(1), 43–54 (1989), [http://dx.doi.org/10.1016/0034-4257\(89\)90046-1](http://dx.doi.org/10.1016/0034-4257(89)90046-1).
22. B. C. Gao, "NDWI: a normalized difference water index for remote sensing of vegetation liquid water from space," *Remote Sens. Environ.* **58**(3), 257–266 (1996), [http://dx.doi.org/10.1016/S0034-4257\(96\)00067-3](http://dx.doi.org/10.1016/S0034-4257(96)00067-3).
23. P. J. Zarco-Tejada, C. A. Rueda, and S. L. Ustin, "Water content estimation in vegetation with MODIS reflectance data and model inversion methods," *Remote Sens. Environ.* **85**(1), 109–124 (2003), [http://dx.doi.org/10.1016/S0034-4257\(02\)00197-9](http://dx.doi.org/10.1016/S0034-4257(02)00197-9).
24. J. B. Féret et al., "PROSPECT-4 and 5: advances in the leaf optical properties model separating photosynthetic pigments," *Remote Sens. Environ.* **112**(6), 3030–3043 (2008), <http://dx.doi.org/10.1016/j.rse.2008.02.012>.

25. S. Jacquemoud et al., "PROSPECT + SAIL models: a review of use for vegetation characterization," *Remote Sens. Environ.* **113**(Supplement 1), S56–S66 (2009), <http://dx.doi.org/10.1016/j.rse.2008.01.026>.
26. J. B. Féret et al., "Optimized spectral indices and chemometric analysis of leaf chemical properties using radiative transfer modeling," *Remote Sens. Environ.* **115**(10), 2742–2750 (2011), <http://dx.doi.org/10.1016/j.rse.2011.06.016>.
27. W. Verhoef, "Light scattering by leaf layers with application to canopy reflectance modeling: the SAIL model," *Remote Sens. Environ.* **16**(2), 125–141 (1984), [http://dx.doi.org/10.1016/0034-4257\(84\)90057-9](http://dx.doi.org/10.1016/0034-4257(84)90057-9).
28. C. J. Willmott, "Some comments on the evaluation of model performance," *Bull. Amer. Meteorol. Soc.* **63**(11), 1309–1313 (1982), [http://dx.doi.org/10.1175/1520-0477\(1982\)063<1309:SCOTEO>2.0.CO;2](http://dx.doi.org/10.1175/1520-0477(1982)063<1309:SCOTEO>2.0.CO;2).
29. B. C. Gao et al., "Atmospheric correction algorithms for hyperspectral remote sensing data of land and ocean," *Remote Sens. Environ.* **113**(Supplement 1), S17–S24 (2009), <http://dx.doi.org/10.1016/j.rse.2007.12.015>.
30. C. S. T. Daughtry et al., "Estimating corn leaf chlorophyll concentration from leaf and canopy reflectance" *Remote Sens. Environ.* **74**(2), 229–239 (2000), [http://dx.doi.org/10.1016/S0034-4257\(00\)00113-9](http://dx.doi.org/10.1016/S0034-4257(00)00113-9).
31. D. Haboudane et al., "Integrated narrow-band vegetation indices for prediction of crop chlorophyll content for application to precision agriculture," *Remote Sens. Environ.* **81**(2–3), 416–426 (2002), [http://dx.doi.org/10.1016/S0034-4257\(02\)00018-4](http://dx.doi.org/10.1016/S0034-4257(02)00018-4).
32. P. J. Zarco-Tejada et al., "Hyperspectral indices and model simulation for chlorophyll estimation in open-canopy tree crops," *Remote Sens. Environ.* **90**(4), 463–476 (2004), <http://dx.doi.org/10.1016/j.rse.2004.01.017>.
33. J. U. H. Eitel et al., "Combined spectral index to improve ground-based estimates of nitrogen status in dryland wheat," *Agron. J.* **100**(6), 1694–1702 (2008), <http://dx.doi.org/10.2134/agronj2007.0362>.
34. P. Ceccato, S. Flasse, and J. M. Grégoire, "Designing a spectral index to estimate vegetation water content from remote sensing data: part 2. Validation and applications," *Remote Sens. Environ.* **82**(2–3), 198–207 (2002), [http://dx.doi.org/10.1016/S0034-4257\(02\)00036-6](http://dx.doi.org/10.1016/S0034-4257(02)00036-6).
35. Y. B. Cheng et al., "Estimating vegetation water content with hyperspectral data for different canopy scenarios: relationships between AVIRIS and MODIS indexes," *Remote Sens. Environ.* **105**(4), 354–366 (2006), <http://dx.doi.org/10.1016/j.rse.2006.07.005>.
36. A. Davidson, S. Wang, and J. Wilmhurst, "Remote sensing of grassland-shrubland vegetation water content in the shortwave domain," *Int. J. Appl. Earth Obs. Geoinform.* **8**(4), 225–236 (2006), <http://dx.doi.org/10.1016/j.jag.2005.10.002>.
37. M. T. Yilmaz et al., "Vegetation water content during SMEX04 from ground data and Landsat 5 Thematic Mapper imagery," *Remote Sens. Environ.* **112**(2), 350–362 (2008), <http://dx.doi.org/10.1016/j.rse.2007.03.029>.
38. M. T. Yilmaz, E. R. Hunt, Jr., and T. J. Jackson, "Remote sensing of vegetation water content from equivalent water thickness using satellite imagery," *Remote Sens. Environ.* **112**(5), 2514–2522 (2008), <http://dx.doi.org/10.1016/j.rse.2007.11.014>.
39. X. Xiao et al., "Characterization of forest types in Northeastern China, using multi-temporal SPOT-4 VEGETATION sensor data," *Remote Sens. Environ.* **82**(2–3), 335–348 (2002), [http://dx.doi.org/10.1016/S0034-4257\(02\)00051-2](http://dx.doi.org/10.1016/S0034-4257(02)00051-2).
40. N. Delbart et al., "Remote sensing of spring phenology in boreal regions: a free of snow-effect method using NOAA-AVHRR and SPOT-VGT data (1982–2004)," *Remote Sens. Environ.* **101**(1), 53–62 (2006), <http://dx.doi.org/10.1016/j.rse.2005.11.012>.
41. F. Gao et al., "On the blending of the Landsat and MODIS surface reflectance: predicting daily Landsat surface reflectance," *IEEE Trans. Geosci. Remote Sens.* **44**(8), 2207–2218 (2006), <http://dx.doi.org/10.1109/TGRS.2006.873336>.

Biographies and photographs of the authors are not available.